Electronic Supplementary Material (ESI) for Sustainable Energy & Fuels.

ELECTRONIC SUPPLEMENTARY INFORMATION

Multi-phase real-time monitoring of oxygen evolution enables *in operando* water oxidation catalysis studies

Fabian L. Huber, Sebastian Amthor, Benjamin Schwarz, Boris Mizaikoff, Carsten Streb* and Sven Rau*

1. Experimental Procedures

Synthesis: [Ru(dpp)(pic)](PF6)2,[1] $[Ru(dceb)_2(bpy)](PF_6)$[2] and $[Mn_4V_4O_{17}(OAc)_3]^{3-}$[3] were prepared according to published syntheses.

Photochemical water oxidation catalysis: all studies were carried out in de-aereated solvents under inert atmosphere. All catalytic experiments were tempered by a custom air cooling setup (25 °C, Fig S1). A screw cap, hermetically sealed vial (diameter: 12.75 ± 0.25 mm, length: 99.00 ± 0.50 mm) equipped with two sensor spots (see "Oxygen detection" below) was used as reaction vessel. The mixtures were not stirred during catalysis, unless mentioned otherwise.

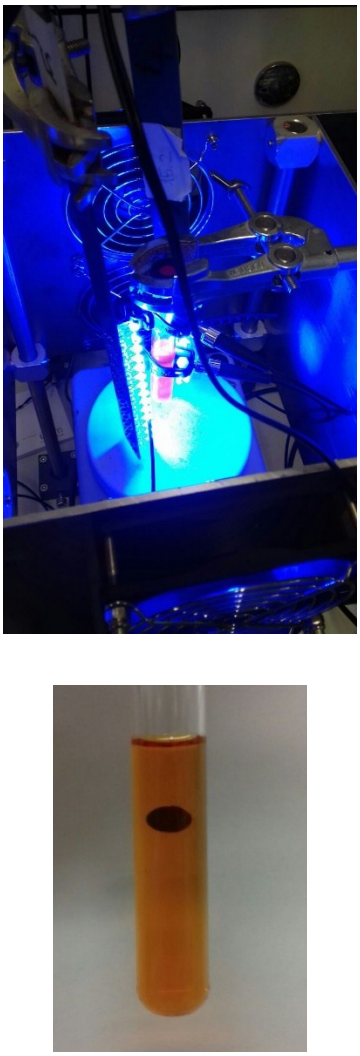

Figure S1. Top: Sealed reaction vessel equipped with oxygen sensor spots, mounted inside in a custom air cooling reactor. Bottom: Catalytic solution, containing $[Ru(dpp)(pic)_2](PF_6)_2$ (2.6 µM) as catalyst and $[Ru(dceb)_2(bpy)](PF_6)_2$ (0.3 mM) as photosensitizer.

Oxygen detection: Oxygen concentrations were determined using a FireStingO2 optical oxygen meter (Pyroscience, Germany) using oxygen sensitive optical sensor spots (OXSP5, with optical isolation). The spots were glued to the inner glass vessel wall of a screw-capped vial (transparent silicone glue, SPGLUE). The sensor spots are stable between pH 1 – 14, stable in the presence of strong oxidants (the manufacturer suggests cleaning in 3 % aqueous $H2O_2$), are not affected by the solvents used (as shown by repeated reproducible catalytic measurements) and are autoclavable at 120 °C. For further information, see the manufacturer information: https://www.pyro-science.com/contactless-fiber-optic-oxygen-sensor-spots.html. O_2 concentration was measured in µmol/L (solution) and mbar (gas-phase). Both spots were calibrated by two-point calibration: gas-phase calibration was performed against ambient air and Ar-atmosphere. Liquid-phase calibration was performed using a de-oxygenated reaction solution (aqueous sodium dithionite for Ru-WOC; de-aerated MeCN/H_2O solution for **{Mn_4V_4}**). Solution *TONs* were calculated based on the detected concentration; gas-phase *TONs* were calculated *via* the ideal gas equation.

Irradiation setup: Irradiation of the samples was performed utilizing two LED-sticks (λ_{max} = 470 nm, power density at the sample *ca.* 50 mW cm^{-2} as determined using a power meter, also see Fig S2). Both sticks were placed on opposite sides of the reaction vessel.

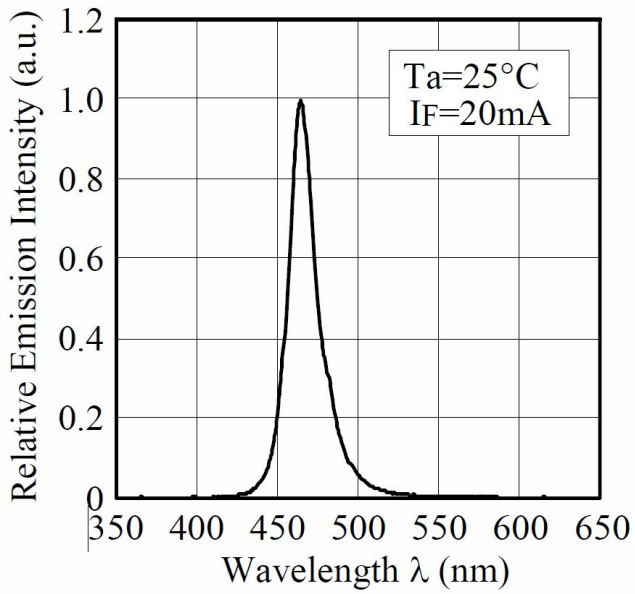

Figure S2. Emission spectrum of the LEDs used as irradiation source.

Ru-WOC catalysis: $[Ru(dpp)(pic)_2](PF_6)_2$ (2.6 µM), photosensitizer (0.3 mM, $[Ru(bpy)2](PF_6)_2$, $[Ru(bpy)_2]Cl_2$ or $[Ru(dceb)_2(bpy)](PF_6)_2$) and $Na_2S_2O_8$ (10 mM) were dissolved in a $Na_2SiF_6/NaHCO_3$ aqueous buffer (pH 6.8, 0.01 M Na_2SiF_6, 5 mL containing 70 µL MeCN). The solutions were kept in sealed glass GC vial equipped with two sensor "spots".

{Mn_4V_4} catalysis: $[Mn_4V_4O_{17}(OAc)_3]^{3-}$ (0.3µM), the photosensitizer (1.0 mM, $[Ru(bpy)_2](PF_6)_2$, $[Ru(bpy)_2]Cl_2$)) and $Na_2S_2O_8$ (10 mM) are dissolved in MeCN/H_2O (9:1, v:v). The homogenous solutions were irradiated with LED light sources (λ_{max} = 470 nm, *ca.* 50 mW cm^{-2}).

2. Turnover Frequencies (*TOFs*) and total O_2 amounts of the studied systems

Turnover frequencies were independently calculated from the *TON*s obtained from the oxygen measurement in the gas and the liquid phase. The total *TOF* is based on the measurements in the gas phase and the solution.

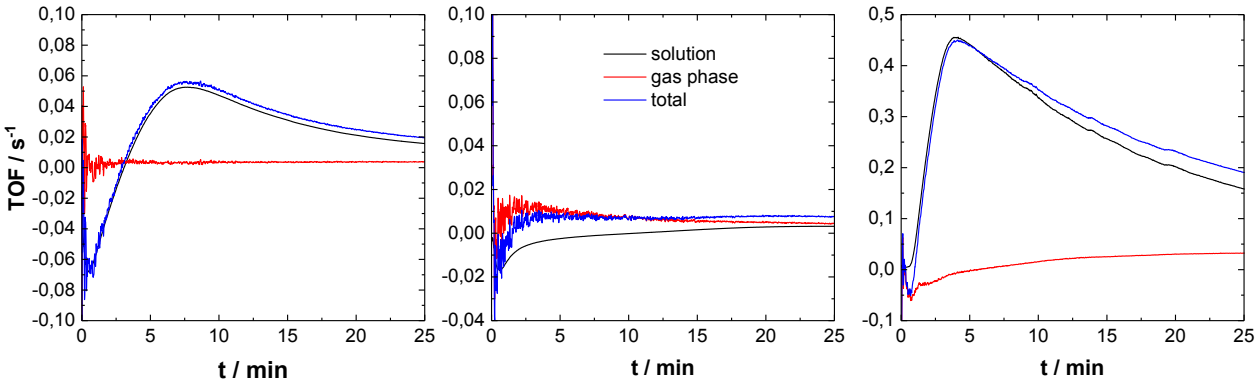

Figure S3. *TOF* of the light-driven oxygen evolution of the **Ru-WOC** system utilizing different photosensitizers. **Left:** $[Ru(bpy)_3](PF_6)_2$. **Center:** $[Ru(bpy)_3]Cl_2$. **Right:** $[Ru(dceb)_2(bpy)](PF_6)_2$. Catalyst *TONs* were calculated based on the oxygen detected in solution and gas phase using eq. 2. Conditions: **Ru-WOC** = 2.6 µM; PS = 0.3 mM; $Na_2S_2O_8$ = 10 mM. Solvent: aqueous Na_2SiF_6/$NaHCO_3$ buffer, pH 6.8, 0.01 M Na_2SiF_6. Irradiation: LED, λ_{max} = 470 nm, *ca.* 50 mW cm^{-2}.

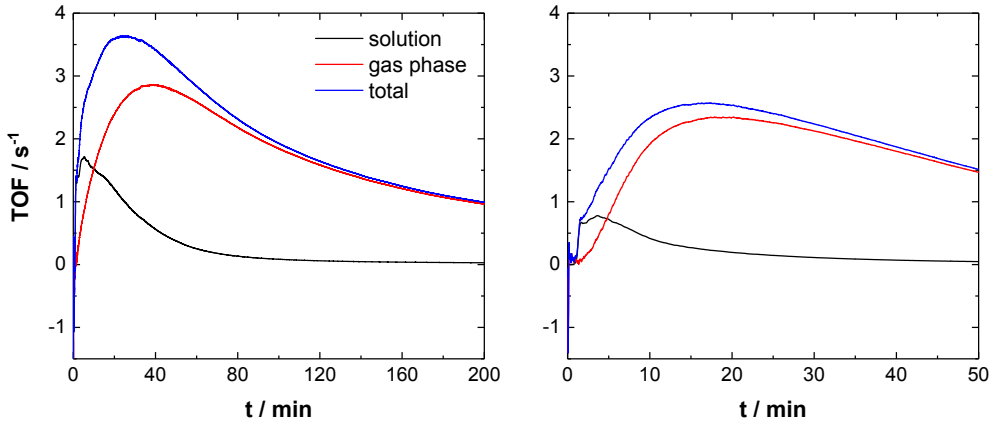

Figure S4. *TOF* of the light-driven O_2 evolution based on measurements in solution and gas-phase for the **{Mn_4V_4}** system. **Left:** chloride-free system using the photosensitizer $[Ru(bpy)_3](\mathbf{PF_6})_2$. **Right:** chloride-containing system using the photosensitizer $[Ru(bpy)_3]\mathbf{Cl}_2$. Conditions: **{Mn_4V_4}** = 0.3 µM, PS = 1 mM, $Na_2S_2O_8$ = 10 mM in MeCN / H_2O (9:1) using LED irradiation (λ_{max} = 470 nm, *ca.* 50 mW cm^{-2}).

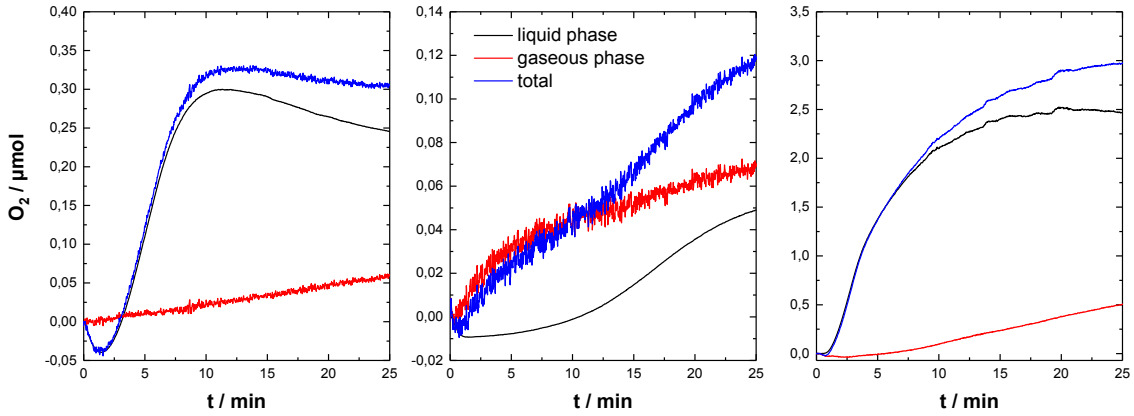

Figure S5. Amount of oxygen produced during light-driven water oxidation of the **Ru-WOC** system utilizing different photosensitizers. **Left:** $[Ru(bpy)_3](PF_6)_2$. **Center:** $[Ru(bpy)_3]Cl_2$. **Right:** $[Ru(dceb)_2(bpy)](PF_6)_2$. Conditions: **Ru-WOC** = 2.6 µM; PS = 0.3 mM; $Na_2S_2O_8$ = 10 mM. Solvent: aqueous $Na_2SiF_6/NaHCO_3$ buffer, pH 6.8, 0.01 M Na_2SiF_6. Irradiation: LED, λ_{max} = 470 nm, *ca.* 50 mW cm^{-2}.

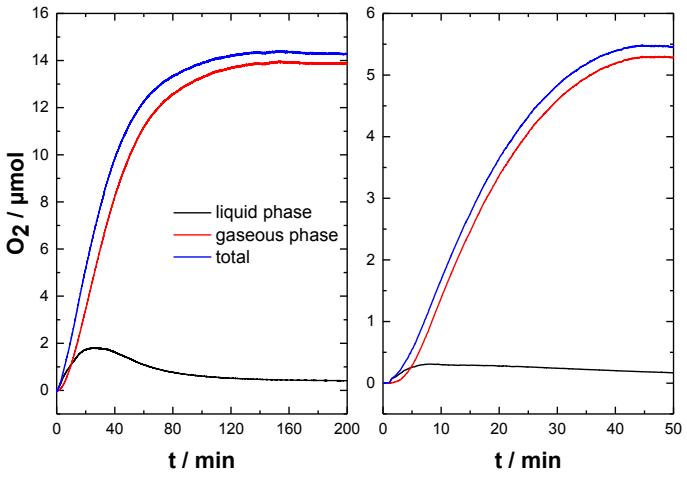

Figure S6. Amount of oxygen produced during light-driven water oxidation based on measurements in solution and gas-phase for the **$\{Mn_4V_4\}$** system. **Left:** chloride-free system using the photosensitizer $[Ru(bpy)_3](\mathbf{PF_6})_2$. **Right:** chloride-containing system using the photosensitizer $[Ru(bpy)_3]\mathbf{Cl}_2$. Conditions: **$\{Mn_4V_4\}$** = 0.3 µM, PS = 1 mM, $Na_2S_2O_8$ = 10 mM in MeCN / H_2O (9:1) using LED irradiation (λ_{max} = 470 nm, *ca.* 50 mW cm^{-2}).

3. Proposed Mechanism of Cl^- Poisoning

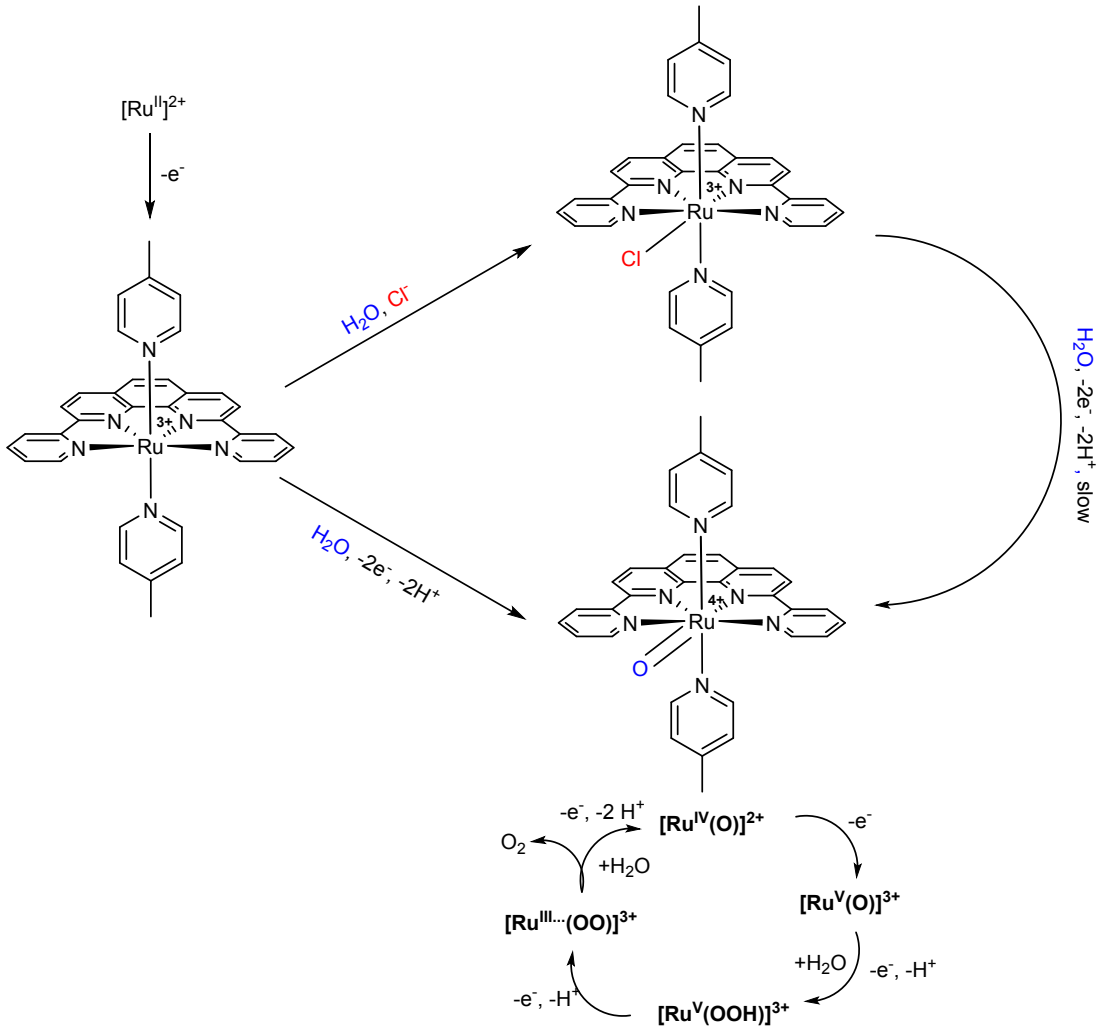

Figure S7. Possible mechanism of poisoning by chloride based on mechanistic studies by Thummel *et al*..[4]

4. Reference Measurements

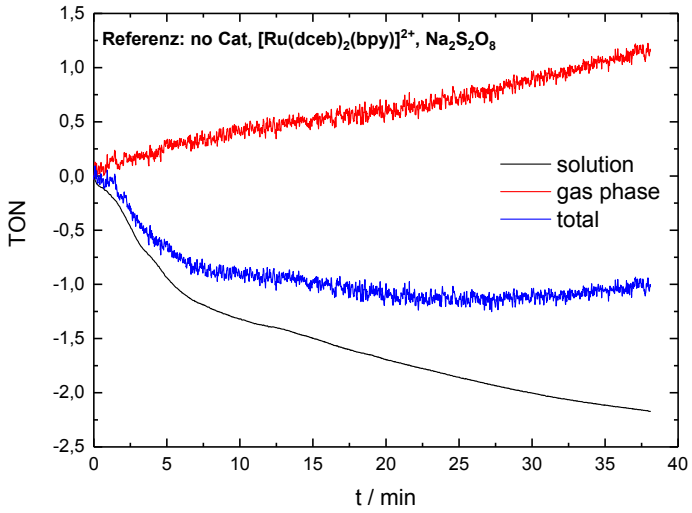

Figure S8. Negligible O_2-evolution upon irradiation of a catalyst-free mixture containing $[(Ru(dceb)_2(bpy)](PF_6)_2$ (0.3 mM) and $Na_2S_2O_8$ (10 mM).

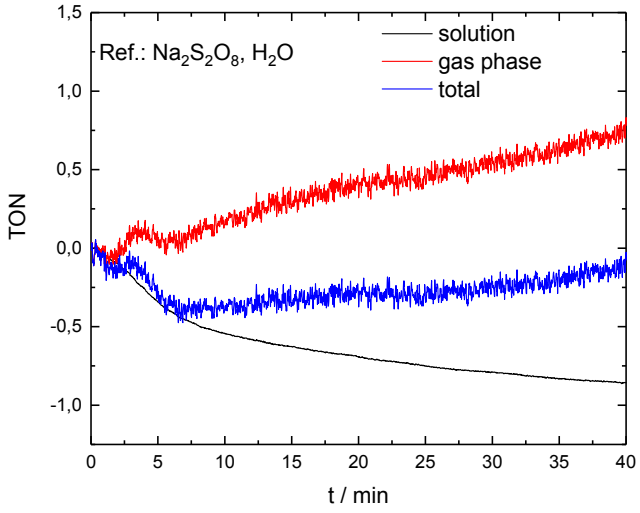

Figure S9. Negligible O_2-evolution upon irradiation of an aqueous $Na_2S_2O_8$ solution (10 mM), containing no catalyst or photosensitizer.

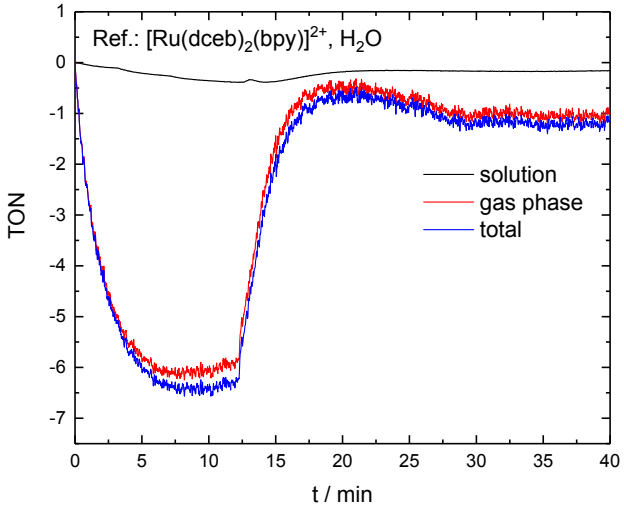

Figure S10. Negligible O_2-evolution upon irradiation of a $[(Ru(dceb)_2(bpy)](PF_6)_2$ solution (0.3 mM) containing no persulfate.

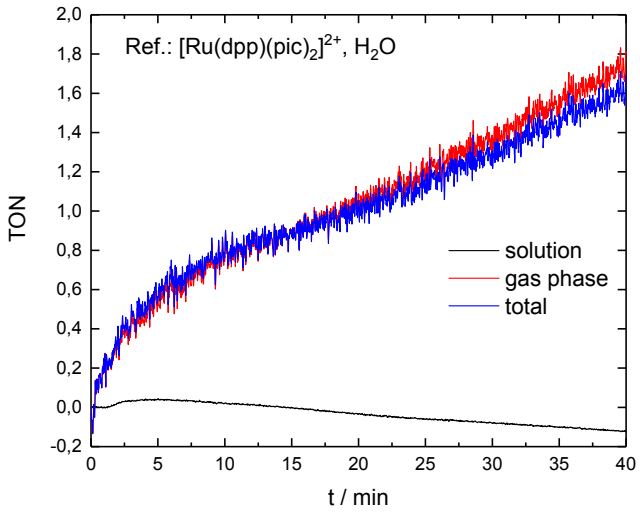

Figure S11. Negligible O_2-evolution upon irradiation of a $[(Ru(dpp)(pic)_2](PF_6)_2$ solution (2.5 µM), with no peroxodisulfate and no photosensitizer.

5. Influence of Stirring

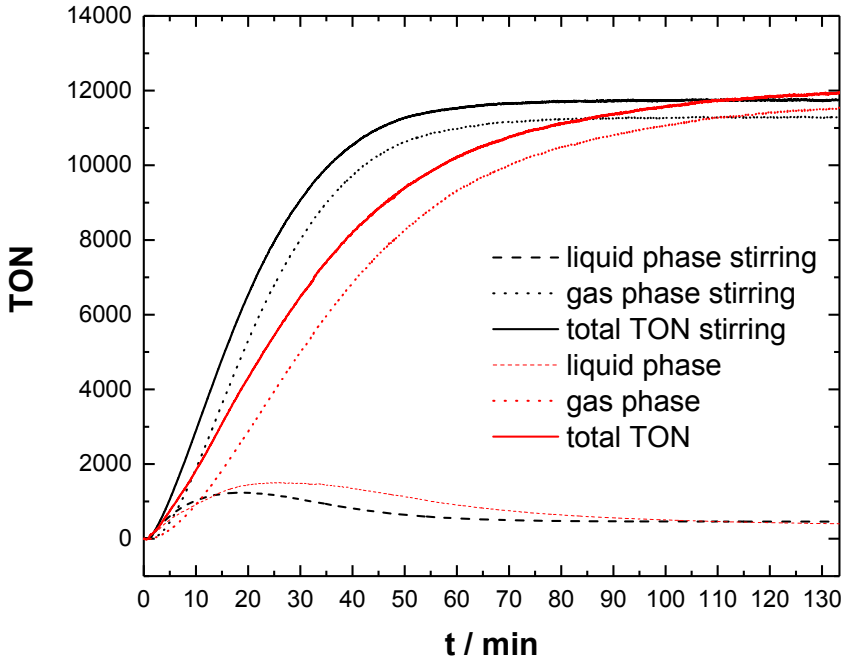

Figure S12. Influence of stirring a catalytic solution of $\{Mn_4V_4\}$ (0.3 µM), $[Ru(bpy)_3](PF_6)_2$ (1 mM) and $Na_2S_2O_8$ (10 mM) in an $MeCN/H_2O$ solution while being irradiated with two blue LED-sticks (λ_{max} = 470 nm, *ca.* 50 mW cm^{-2}).

6. Reproducability

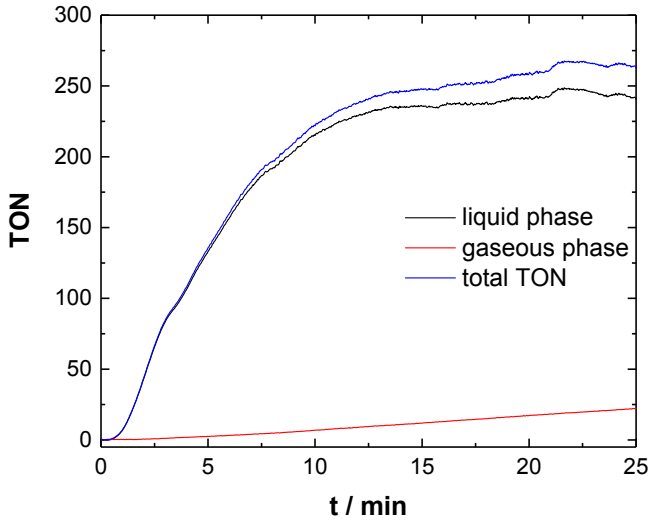

Figure S13. Light-driven oxygen evolution of the **Ru-WOC** system utilizing $[Ru(dceb)_2(bpy)](PF_6)_2$ as photosensitizer. Conditions: $[Ru(dpp)(pic)_2](PF_6)_2$ = 2.6 µM, PS = 0.3 mM, $Na_2S_2O_8$ = 10 mM. Solvent: aqueous $Na_2SiF_6/NaHCO_3$ buffer, pH 6.8, 0.01 M Na_2SiF_6. Irradiation: two LED-sticks, λ_{max} = 470 nm, *ca.* 50 mW cm^{-2}).

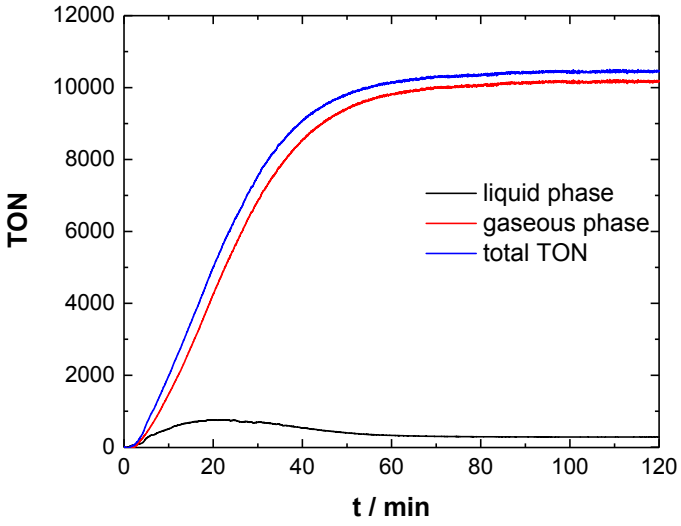

Figure S14. Light-driven O_2 evolution in solution and gas-phase for the **$\{Mn_4V_4\}$** system utilizing $[Ru(bpy)_3](PF_6)_2$ as photosensitizer. Conditions: **$\{Mn_4V_4\}$** = 0.3 µM, PS = 1 mM, $Na_2S_2O_8$ = 10 mM in MeCN/H_2O (9:1) using LED irradiation (λ_{max} = 470 nm, *ca.* 50 mW cm^{-2}).

7. Literature

1 G. Zhang, R. Zong, H. W. Tseng and R. P. Thummel, *Inorg. Chem.*, 2008, **47**, 990–998.

2 T. Kowacs, L. O'Reilly, Q. Pan, A. Huijser, P. Lang, S. Rau, W. R. Browne, M. T. Pryce and J. G. Vos, *Inorg. Chem.*, 2016, **55**, 2685–2690.

3 B. Schwarz, J. Forster, M. K. Goetz, D. Yücel, C. Berger, T. Jacob and C. Streb, *Angew. Chem. Int. Ed.*, 2016, **55**, 6329–6333.

4 J. T. Muckerman, M. Kowalczyk, Y. M. Badiei, D. E. Polyansky, J. J. Concepcion, R. Zong, R. P. Thummel and E. Fujita, *Inorg. Chem.*, 2014, **53**, 6904–6913.